RetinaCAD, a System for the Assessment of Retinal Vascular Changes*

Behdad Dashtbozorg[1], Ana Maria Mendonça[2], *IEEE Senior Member*, Susana Penas[3], and Aurélio Campilho[4], *IEEE Member*

***Abstract*— This paper introduces RetinaCAD, a system, for the fast, reliable and automatic measurement of the Central Retinal Arteriolar Equivalent (CRAE), the Central Retinal Venular Equivalent (CRVE), and the Arteriolar-to-Venular Ratio (AVR) values, as well as several geometrical features of the retinal vasculature. RetinaCAD identifies important landmarks in the retina, such as the blood vessels and optic disc, and performs artery/vein classification and vessel width measurement. The estimation of the CRAE, CRVE and AVR values on 480 images from 120 subjects has shown a significant correlation between right and left eyes and also between images of same eye acquired with different camera fields of view. AVR estimation in retinal images of 54 subjects showed the lowest values in people with diabetes or high blood pressure thus demonstrating the potential of the system as a CAD tool for early detection and follow-up of diabetes, hypertension or cardiovascular pathologies.**

I. Introduction

Changes in the retinal vessels is recognized as a relevant consequence of several systemic diseases. In conditions such as diabetic retinopathy, the blood vessels often show abnormalities at early stages. Changes in retinal blood vessels are also associated with hypertension and other cardio-vascular conditions. Among other features associated with vascular changes, the Central Retinal Arteriolar Equivalent (CRAE), the Central Retinal Venular Equivalent (CRVE) and the Arteriolar-to-Venular Ratio (AVR) have been frequently used as indicators for the early detection, diagnosis, staging and follow-up of diabetes and hypertension, since they can reflect the narrowing or dilation of the retinal blood vessels [1], [2]. These diseases also change the pattern of vessel branching, thus making the measurement of bifurcation geometrical features a useful tool for the diagnosis or prediction of such pathologic conditions [3].

*This work was supported by FEDER funds through the Programa Operacional Factores de Competitividade-COMPETE and by Portuguese funds through FCT - Fundação para a Ciência e a Tecnologia in the framework of the project PEst-C/SAU/LA0002/2013 and the research grant SFRH /BD/73376/2010.

[1]B. Dashtbozorg is with INEB - Instituto de Engenharia Biomédica and also with the Faculdade de Engenharia, Universidade do Porto, Campus da FEUP, Rua Dr. Roberto Frias, 4200-465 Porto, Portugal behdad.dashtbozorg@fe.up.pt

[2]A. M. Mendonça is with INEB - Instituto de Engenharia Biomédica and also with the Faculdade de Engenharia, Universidade do Porto, Campus da FEUP, Rua Dr. Roberto Frias, 4200-465 Porto, Portugal amendon@fe.up.pt

[3]S. Penas is with Centro Hospitalar São João and also with FMUP - Faculdade de Medicina, Universidade do Porto, Porto, Portugal susanaapenas@gmail.com

[4]A. Campilho is with INESC TEC - INESC Science and Technology and also with the Faculdade de Engenharia, Universidade do Porto, Campus da FEUP, Rua Dr. Roberto Frias, 4200-465 Porto, Portugal campilho@fe.up.pt

The main goal of this work is the development of an automatic system for analysing retinal images aiming at the estimation of features useful for the early detection and diagnosis of diabetes, hypertension or cardiovascular pathologies. From the ophthalmologic point of view, this system is also relevant for assessing the implications of such diseases in the eye, as well as to evaluate the response of patients to specific therapeutic approaches. Several semi-automatic retinal image analysis systems have been proposed but the development of a fully automatic system for the assessment of vascular changes is still open.

In this paper, we describe the image analysis tools available in the Retinal Computer Aided Diagnosis (RetinaCAD) system, namely vessel segmentation, vessel width estimation, artery/vein (A/V) classification and optic disc segmentation. A pipeline of these methods allows the computation of some relevant vessel related indexes, namely CRAE, CRAE and AVR, as well as various geometrical features associated with vessel bifurcations. The evaluation of the system on images of a dataset from a local hospital shows a low failure rate and a significant correlation between the values calculated for distinct images of both eyes of the same patient.

This paper is organized as follows. Section II describes the RetinaCAD system and the tools available in the framework of the application. Experimental results and conclusions are presented in sections III and IV, respectively.

II. RetinaCAD Application

The RetinaCAD is a fully automatic system for the segmentation and classification of retinal structures and for the measurement of vascular features. This system can analyse optic disc centered retinal images with variable resolution and camera field of view (FOV). Fig. 1 shows the main interface of this application. In this section, we briefly describe the tools for the detection and classification of retinal structures that were implemented in the RetinaCAD application.

A. RetinaCAD Image Analysis Tools

The main retinal image analysis tools provided by this application are: 1) vessel segmentation; 2) vessel centerline extraction; 3) optic disc localization; 4) optic disc segmentation; 5) graph representation of the vascular tree; 6) A/V vessel classification; 7) ROI determination.

1) Vessel Segmentation Tool: This tool is used for finding the vessels, and is the first stage for vessel caliber estimation and initial optic disc (OD) localization. The methods described in [4] and [5] are applied for vessel segmentation.

978-1-4244-7929-0/14/$26.00 ©2014 IEEE

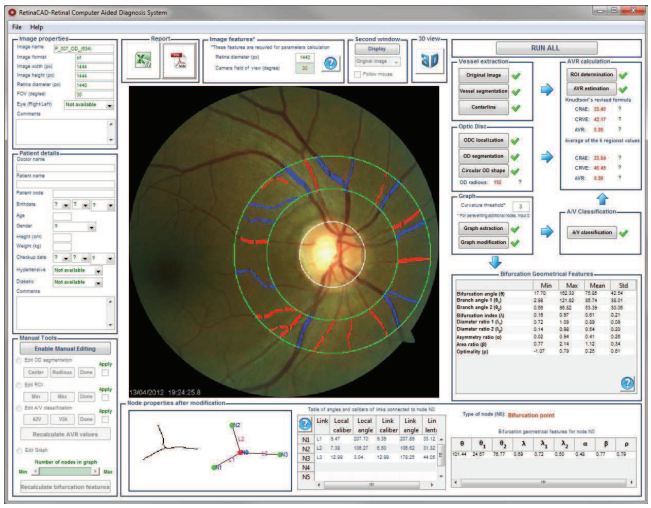

Fig. 1. RetinaCAD interface.

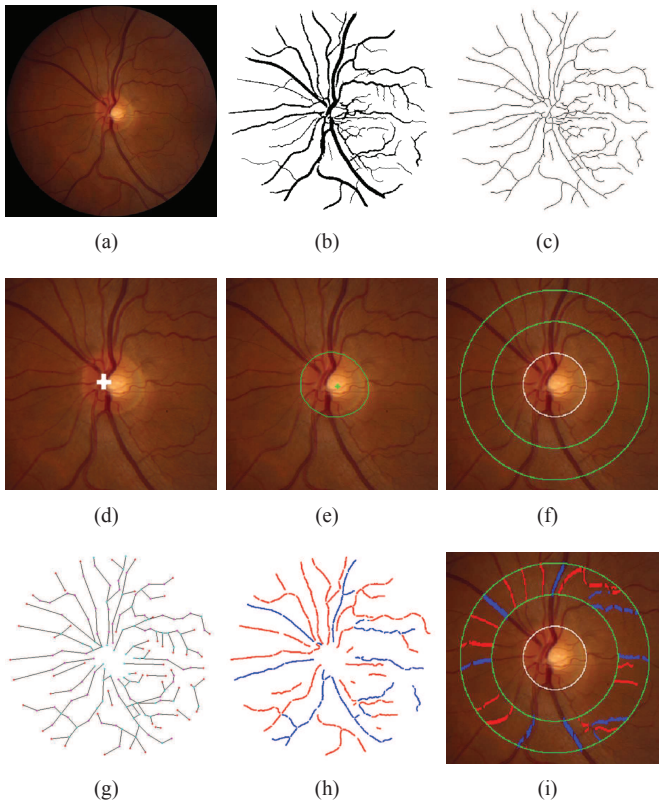

Fig. 2. (a) Input image; (b) Vessel segmentation result; (c) Centerline image; (d) Initial OD location (white cross); (e) OD segmentation; (f) ROI (delimited by the two green circles) and circular OD margin (white circle); (g) Graph representation of vascular tree; (h) A/V classification result; (i) Arteries and veins inside the ROI.

Fig. 2(b) illustrates the vascular tree which is generated by the tool for the original image of Fig. 2(a). Vessel caliber measurement is based on the distance transform of the segmented vascular tree; the result of this transform in each vessel pixel is its distance to the closest boundary point, d. After that, for each vessel centerline pixel, the vessel caliber value, vc, is estimated by $vc = 2d - 1$.

2) Centerline Extraction Tool: The vessels centerline image is obtained by applying an iterative thinning algorithm described in [6] to the vessel segmentation result. This algorithm removes border pixels until the object shrinks to a minimally connected stroke (Fig. 2(c)).

3) Optic Disc Localization Tool: The initial optic disc (OD) location is obtained following the approach based on the entropy of vascular directions in [7] (Fig. 2(d)).

4) Optic Disc Segmentation Tool: A multiresolution sliding band filter (SBF), centered in the initial OD location is used for segmenting the OD boundary [8]. The final optic disc center (ODC) and OD radius are found by fitting a circle to the extracted boundary (Fig. 2(e) and 2(f), respectively).

5) Region of Interest Tool: The CRAE, CRVE and AVR values are calculated from the calibers of the vessels inside a specific region of interest (ROI), defined as the standard ring sector centered on the ODC, within 2 to 3 disc radius from the OD margin [2]. The corresponding ROI for CRAE, CRVE and AVR calculation is shown in Fig. 2(f).

6) Graph Representation Tool: Graph nodes are extracted from the centerline image by finding the intersection points, the bifurcation points and the terminal points. After that each vessel segment is represented by a link between two nodes (Fig. 2(g)). The graph representation tool can display local and global features of the links (vessel segments) and nodes (bifurcation/intersection points), namely the caliber and the angle between vessel segments as well as the type of intersection (crossing or bifurcation).

7) Artery/Vein Classification Tool: This tool is based on the graph representation of the retinal vasculature as described in [9]. This method classifies the entire vascular tree by deciding on the type of each vessel intersection point (graph nodes) and by assigning one of two labels to each vessel segment (graph links). Final classification of a vessel segment as an artery or a vein is performed through the combination of the graph-based labeling results with a set of intensity features. The results of A/V classification for the whole image and inside the ROI are shown in Fig. 2(h) and Fig. 2(i), respectively.

B. Measurements

In addition to the measurement of vessel caliber and OD radius, this application automatically computes several vascular features, namely the CRAE, CRVE, AVR, bifurcation index, asymmetry ratio, diameter ratio, area ratio and optimality.

1) CRAE, CRVE and AVR Computation: The CRAE and CRVE values are calculated based on Knudtson's revised formulas [2] for the calculation of the equivalent width of two vessel branches

$$Arterioles : \hat{W}_a = 0.88 * \left({w_{a1}}^2 + {w_{a2}}^2\right)^{\frac{1}{2}} \quad (1)$$

$$Venules : \hat{W}_v = 0.95 * \left({w_{v1}}^2 + {w_{v2}}^2\right)^{\frac{1}{2}} \quad (2)$$

where w_{a1} , w_{a2}, and $\hat{W}_a$ are, respectively, the width of the narrowest artery, the width of the widest artery, and the

estimate of parent trunk for those arteries; w_{v1}, w_{v2}, and $\hat{W}_v$ have similar meanings for veins.

For computing the CRAE, a set with the six largest arteries inside the ROI is first selected. Then, the largest and the smallest vessels in this set are paired up, and the parent trunk width is determined using Knudtson's formula. A new set is formed by substituting the largest and smallest arteries with the parent trunk, and this algorithm is iterated until a single vessel is kept, whose width is the CRAE value. A similar procedure is used for calculating the CRVE. The AVR is defined as the quotient between CRAE and CRVE. For the AVR calculation, the ROI is equidistantly sampled to provide six regions. For each region, the six largest arteries and the six largest veins are identified, and the regional AVR is calculated. The final AVR estimate for the complete image is the average of the six regional values.

2) Computation of the Bifurcation Features: In each bifurcation, we consider a trunk vessel and two branches, the largest and the smallest, with diameters d_0, d_1, and d_2, respectively. The branching angles are the basic measurements related to a bifurcation, and these features are obtained from the graph representing the vascular tree, as mentioned before. At each bifurcation, the branching angles and vessel segment calibers are used for deriving features, such as

- Bifurcation angle (θ): angle between the smaller and larger branches.
- Bifurcation index (λ): quotient between the diameter of the smaller and larger branches.

$$\lambda = d_2/d_1 \tag{3}$$

- Asymmetry ratio (α): cross-sectional area of the smaller branch divided by that of the larger.

$$\alpha = d_2^2/d_1^2 \tag{4}$$

- Diameter ratios (λ_1, λ_2): branches diameter divided by trunk diameter.

$$\lambda_1 = d_1/d_0, \quad \lambda_2 = d_2/d_0 \tag{5}$$

- Area ratio (β): sum of cross-sectional areas of two branches divided by that of the trunk.

$$\beta = \left(d_1^2 + d_2^2\right)/d_0^2 \tag{6}$$

- Optimality (ρ): deviation of the junction power law value from the optimal value.

$$\rho = \left[d_0^3 - \left(d_1^3 + d_2^3\right)\right]^{1/3}/d_0 \tag{7}$$

C. Additional Features

In order to increase interactivity and usability, RetinaCAD offers additional features and tools, namely: 1) single click option for the CRAE, CRVE and AVR estimation; 2) visualization of intermediate and final results; 3) the ability to process an individual task; 4) display of vessel bifurcation/intersection (graph node) features using a mouse click; 5) availability of a *follow mouse* tool using a second display window for comparison purposes; 6) generation of reports in PDF or Excel files. Tools for manual modification of several calculated results are also available, namely for changing the ODC location, the OD radius value, the ROI, single vessel A/V classification and the number of nodes in the graph.

TABLE I

COMPARISON OF MEAN ± STANDARD DEVIATION (SD) AND PEARSON CORRELATION BETWEEN IMAGES OF THE RIGHT AND LEFT EYES.

Measurements	RetinaCAD Mean ± SD		RetinaCAD Mean error±SD	RetinaCAD Corr.	BDES [10] Corr.	Leung [11] Corr.
	Right eye	Left eye				
CRAE (μm)	148.0±14.4	156.1±12.9	10.0±7.5	0.71	0.71	0.70
CRVE (μm)	246.7±23.4	248.8±24.0	13.8±11.4	0.72	0.74	0.77
AVR	0.61±0.07	0.62±0.07	0.06±0.04	0.51	0.49	0.54

Corr.: Pearson's correlation coefficient.

III. EXPERIMENTAL VALIDATION

The system was evaluated using the images of a dataset from Centro Hospitalar São João (CHSJ dataset). This dataset contains 528 images from 132 subjects, where for each subject there are four images, two from the right eye and two from the left eye; the two images of each eye were acquired with two different FOV values (45° and 30°).

The images of this dataset were used for investigating the robustness of the system to the use of distinct images of the same subject, through the assessment of the correlation between measurements from images of the right and left eyes and from images of same eye with different FOV. For the 528 images that were analysed using RetinaCAD, the results for 25 images were not accepted as a consequence of errors in A/V classification or OD segmentation. Although these errors can be solved using the manual modification tool which is included in this application, all the images of the subjects where the automatic procedures have failed (12 subjects) were excluded. In the following, we discuss the results obtained for 480 images from 120 subjects.

The mean error and the Pearson correlation coefficient between measurements from the right and left eyes in the CHSJ dataset are shown in Table I, where the correlation coefficients reported by the Beaver Dam Eye Study (BDES) [10] and Leung *et al.* [11] are also included. These results show a good correlation between right and left eyes for CRAE and CRVE and a moderate correlation for AVR, being similar to those reported in [10] and [11].

In order to evaluate the robustness of the methods in RetinaCAD, we have compared the results of the CRAE, CRVE and AVR values in images of the same eye that were acquired with a different FOV (45° and 30°). A mean error of 5.9 pixels (37.6 μm) and a relative error of 4% were achieved for the estimated OD radius when the 45° FOV and 30° FOV images were compared. For the same set of images, the Pearson correlation coefficient and mean error for the CRAE, CRVE and AVR values are shown in Table II. As can be observed, all indicators show a small mean error and there is a significant correlation between images of the same eye that were acquired in distinct conditions, thus indicating the good performance and consistency of RetinaCAD.

TABLE II

COMPARISON OF RESULTS BETWEEN IMAGES OF THE SAME EYE WITH 45° AND 30° FOV.

Measurements	Mean ± SD		Mean error±SD	Correlation coefficient
	FOV: 45°	FOV: 30°		
CRAE (μm)	144.3±15.5	156.1±12.9	12.7±8.7	0.79
CRVE (μm)	238.9±22.3	257.3±21.9	19.8±12.1	0.79
AVR	0.61±0.07	0.61±0.07	0.04±0.04	0.67

TABLE III

MEAN ± SD OF AVR VALUES FOR THE SUBJECTS IN DIFFERENT CATEGORIES OF BLOOD PRESSURE AND DIABETIC STATUS.

Blood Pressure	Diabetes	Number of subjects	Mean ± SD AVR
Normal	No	22	0.64±0.06
High	No	10	0.62±0.06
Normal	Yes	9	0.63±0.04
High	Yes	13	0.59±0.07

TABLE IV

THE AVERAGE RUNNING TIME OF EACH INDIVIDUAL PROCESS IN RETINACAD.

		CHSJ	CHSJ
	Size	1620 × 1444	2196 × 1958
	FOV	30°	45°
Process time (second)	Vessel segmentation	3.47	8.86
	OD localization	4.30	12.54
	OD segmentation	3.34	3.89
	ROI determination	0.44	0.79
	Graph generation	1.44	4.51
	A/V classification	3.28	11.72
	Features computation	3.22	6.95
	Total	19.49	49.26

Table III shows the mean and standard deviation of the AVR values for 54 subjects with available clinical information. The subjects are categorized in four groups based on the blood pressure (BP) and the risk of diabetes. In this preliminar study with a limited set of subjects, and as can be observed in Table III, the mean AVR value of 0.64 in the non-diabetic people with normal BP is higher than other groups with diabetes and/or high BP, which is in accordance with the association of the AVR value with the risk of diabetes and hypertension.

The RetinaCAD was evaluated on an Intel CPU i7-2600k, 3.40 GHz, 8 GB RAM computer. The average running time of each individual process for the images CHSJ datasets are shown in Table IV.

IV. CONCLUSIONS

We have developed a user-friendly system, RetinaCAD, that is able to automatically detect, measure and classify two main retinal landmarks, the optic disc and the vessels. RetinaCAD can measure several vascular features that are recognized as indicators for some prevalent systemic diseases. This application was assessed in the images of the CHSJ dataset, where it showed an association between AVR values and clinical information of 54 subjects. The lower AVR values in the people with diabetes or high blood pressure in contrast to the non-diabetic ones with normal blood pressure demonstrates the potential of the system as a CAD tool for early detection and follow-up of diabetes, hypertension or cardiovascular pathologies.

We have also demonstrated that the correlation between right and left eyes was good for the CRAE and CRVE values, which suggests that the measurements from one eye can provide adequate information about the changes in vessel calibers. After comparing the measured values for images of the same eye but with different FOV, a significant correlation and a low mean error were achieved, thus allowing the conclusion that RetinaCAD is adequate both for research and for general clinical use.

ACKNOWLEDGMENT

The authors would like to thank Professor Jorge Polónia from Faculdade de Medicina, Universidade do Porto, for making the clinical data available.

REFERENCES

[1] N. Patton, T. Aslam, T. MacGillivray, A. Pattie, I. J. Deary, and B. Dhillon, "Retinal vascular image analysis as a potential screening tool for cerebrovascular disease: a rationale based on homology between cerebral and retinal microvasculatures," *Journal of anatomy*, vol. 206, no. 4, pp. 319–348, 2005.

[2] M. Knudtson, K. Lee, L. Hubbard, T. Wong, R. Klein, and B. Klein, "Revised formulas for summarizing retinal vessel diameters." *Current eye research*, vol. 27, pp. 143–149, 2003.

[3] B. Al-Diri, A. Hunter, D. Steel, and M. Habib, "Manual measurement of retinal bifurcation features." in *in Proc. Engineering in Medicine and Biology Society (EMBC)*, Jan. 2010, pp. 4760–4764.

[4] A. Mendonça and A. Campilho, "Segmentation of retinal blood vessels by combining the detection of centerlines and morphological reconstruction," *IEEE Trans. Med. Imag.*, vol. 25, pp. 1200–1213, Sep. 2006.

[5] A. Mendonça, B. Dashtbozorg, and A. Campilho, "Segmentation of the vascular network of the retina," in *Image Analysis and Modeling in Opthalmology*, E. Y. K. Ng, U. R. Acharya, A. Campilho, and J. S. Suri, Eds. CRC Press, 2014, pp. 85–109.

[6] Z. Guo and R. W. Hall, "Parallel thinning with two-subiteration algorithms," *Communications of the ACM*, vol. 2, no. 3, pp. 359–373, 1989.

[7] A. Mendonça, F. Cardoso, A. Sousa, and A. Campilho, "Automatic localization of the optic disc in retinal images based on the entropy of vascular directions." in *Image Analysis and Recognition*, ser. Lecture Notes Comput. Sci., 2012, vol. 7325, pp. 424–431.

[8] B. Dashtbozorg, A. Mendonça, and A. Campilho, "Optic disc segmentation using the sliding band filter." *IEEE Trans. Med. Imag.*, (submitted).

[9] B. Dashtbozorg, A. M. Mendonça, and A. Campilho, "An automatic graph-based approach for artery/vein classification in retinal images," *IEEE Trans. on Imag. Process.*, vol. 23, no. 3, pp. 1073–1083, March 2014.

[10] T. Y. Wong, M. D. Knudtson, R. Klein, B. E. K. Klein, S. M. Meuer, and L. D. Hubbard, "Computer-assisted measurement of retinal vessel diameters in the Beaver Dam Eye Study: methodology, correlation between eyes, and effect of refractive errors." *Ophthalmology*, vol. 111, no. 6, pp. 1183–90, Jun. 2004.

[11] H. Leung, M. Hons, J. Jin, W. Mmed, E. R. Mapplstat, A. G. T. Hons, T. Y. W. Frcs, L. D. H. Mat, R. K. Mph, and P. M. Franzco, "Clinical and Epidemiological Computer-assisted retinal vessel measurement in an older population: correlation between right and left eyes," *Clinical and Experimental Ophthalmology*, pp. 326–330, 2003.